SEMICONDUCTOR NANOWIRE-BASED FETs AS ELECTRONICALLY TUNABLE CATALYSTS

M. Moskovits*, Y.X. Zhang, Y. Lilach and A. Kolmakov

Department of Chemistry and Biochemistry and the Materials Research Laboratory and the California Nanosystems Institute, University of California Santa Barbara, 93106

ABSTRACT

Nanowires and nanotubes have shown remarkable electronic properties when configured either as simple current/voltage impedance elements or as field-effect transistors. Their very high surface-to-volume ratio makes them ideal sensors in situations where the gaseous species adsorbing on their surface donate or extract charge, in turn affecting the nanowire's conductivity. By reversing the process, nanowires configured as FETs potentially allow the surface chemistry, and hence the catalytic properties of the nanowire, to be tuned using the gate voltage as a kind of chemical-potential-setting parameter. An exciting goal is to use functionalized single-nanowire FETs or devices based on nanowire arrays as systems on whose surface not only the rate and extent of a catalytic reaction but also its selectivity can be varied entirely by varying the voltages applied to the device's terminals.

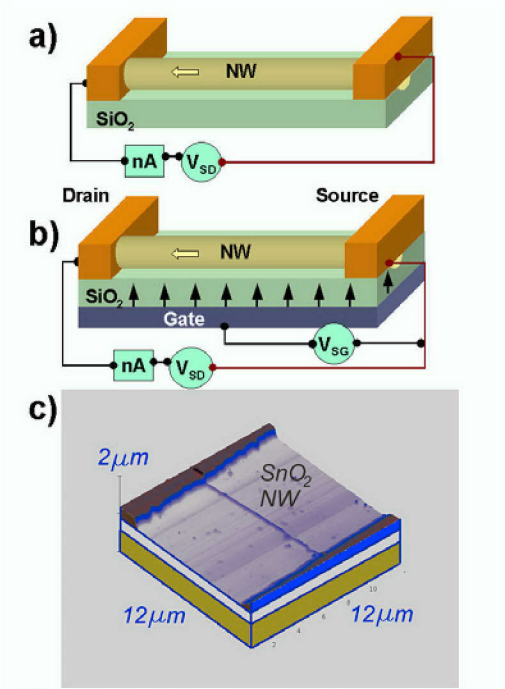

Figure 1. SnO_2 NW configured as (a) a resistor, (b) FET and (c) AFM image of nanowire FET

1. INTRODUCTION

Semiconductor nanowires are poised to impact on such varied technologies as electronics and opto-electronic, lasers, solar energy conversion, environmental sensing and catalysis [1-6]. Their large surface to volume ratio and their function as quasi-one-dimensional conductive elements simultaneously confer upon them high sensitivity and size-dependent transduction of the chemical processes occurring at their surface into functional electrical signals. Significant progress has already been reported involving carbon nanotubes and semiconductor nanowires [7-10] as sensors and in other electronic applications. Contrariwise, the fabrication of devices based on metal oxide nanowires is still largely undeveloped [3,4,11,12] despite the fact that metal-oxides are widely used as support materials for "real world" catalysts and as gas sensors[13-17].

In this communication we report the successful fabrication of a two terminal (Chemoresistor) and three terminal source-gate-drain single-nanowire field-effect transistor (Chem-FET) devices operating as active catalytic and gas sensing elements (Fig.1). We demonstrate that routine manufacturing of these devices can be accomplished using template-synthesis, as well as chemical vapor growth. Their function will be illustrated with SnO_2 nanowires whose electron transport is explored as a function of temperature, gas environment and gate potential.

We find that chemisorption of oxidants (such as oxygen) as well as interactions with reducing gases (like CO) can greatly change the electron density inside the nanowire. Reciprocally, oxygen adsorptivity can be controlled and, as a result, the subsequent catalytic conversion of CO to CO_2 at the SnO_2 surface can be significantly altered upon modulating the electronic state of the material by applying an appropriate gate potential. In close analogy with processes taking place in macroscopic MOSFET gas sensors, [18,19] these observations immediately brings to mind ultra miniature single-nanowire-based FET gas sensors wherein the gate-tunable redox potential controls the sensitivity and selectivity of the surface towards a particular analyte. Reciprocally, the observation implies the possibility of gate-tunable catalysts whose species-selective reactivity, sensitivity and response time can be electronically controlled.

Report Documentation Page

Form Approved
OMB No. 0704-0188

1. REPORT DATE	2. REPORT TYPE	3. DATES COVERED
00 DEC 2004	**N/A**	**-**

4. TITLE AND SUBTITLE	5a. CONTRACT NUMBER
Semiconductor Nanowire-Based Fets As Electronically Tunable Catalysts	5b. GRANT NUMBER
	5c. PROGRAM ELEMENT NUMBER
6. AUTHOR(S)	5d. PROJECT NUMBER
	5e. TASK NUMBER
	5f. WORK UNIT NUMBER
7. PERFORMING ORGANIZATION NAME(S) AND ADDRESS(ES) **Department of Chemistry and Biochemistry and the Materials Research Laboratory and the California Nanosystems Institute, University of California Santa Barbara, 93106**	8. PERFORMING ORGANIZATION REPORT NUMBER
9. SPONSORING/MONITORING AGENCY NAME(S) AND ADDRESS(ES)	10. SPONSOR/MONITOR'S ACRONYM(S)
	11. SPONSOR/MONITOR'S REPORT NUMBER(S)

12. DISTRIBUTION/AVAILABILITY STATEMENT
Approved for public release, distribution unlimited

13. SUPPLEMENTARY NOTES
See also ADM001736, Proceedings for the Army Science Conference (24th) Held on 29 November - 2 December 2004 in Orlando, Florida., The original document contains color images.

14. ABSTRACT

15. SUBJECT TERMS

16. SECURITY CLASSIFICATION OF:			17. LIMITATION OF ABSTRACT	18. NUMBER OF PAGES	19a. NAME OF RESPONSIBLE PERSON
a. REPORT **unclassified**	b. ABSTRACT **unclassified**	c. THIS PAGE **unclassified**	**UU**	**7**	

2. RESULTS AND DISCUSSION

2.1 Experimental

The nanowires used in this research were prepared using two different synthetic methods. In first, (Fig.2 (a)) arrays of parallel tin nanowires with pre-defined, dimensionally uniform diameters and lengths were electrochemically synthesized inside the pores of highly-ordered porous anodic alumina (PAO) templates as previously described [20-24]. Highly crystalline, metallic β-Sn nanowires (60 nm average di. and average length

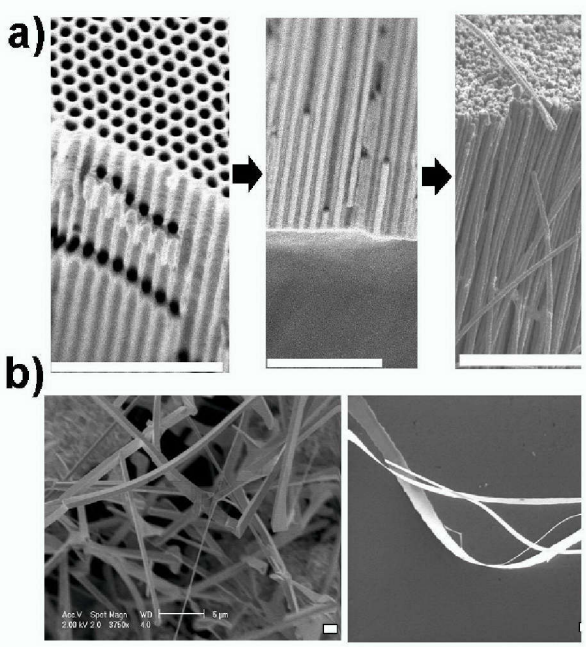

Figure 2. Two approaches for large-scale fabrication of semiconductor metal oxide nanowires. (a) Tin nanowires are grown inside a porous aluminum oxide template. The oxide matrix is removed and the tin nanowires thermally oxidized to SnO_2; (b) SnO_2 nanowires, nanorods and nanobelts are grown by CVD using so-called vapor-solid synthesis.

determined by the template thickness ~ 50 μm in this study) were electrochemically grown in pores of the templates and subsequently removed from their matrix, suspended in a solvent, diluted and deposited on a p-Si (boron doped 0.02 Ω cm) substrate covered with a 300 nm thermally grown SiO_2 film. Individual Sn nanowires were topotactically oxidized to SnO_2 by annealing in air over several hours at several gradually increasing temperature steps eventually reaching 550° C[25]. Transmission electron microscopy (TEM) and X-ray diffraction (XRD) analysis confirmed the nanowire integrity after oxidation and its complete oxidation to (rutile) polycrystalline SnO_2 with crystalline domains (~10^2-10^3 nm) greatly exceeding the nanowire's diameter. Nanowires of higher crystallinity (Fig.2 (b)) were also grown using chemical vapor deposition. [2,26]

Electrical contact to the nanowires was made by vapor-depositing composite Ti (20 nm)/Au (200 nm) micro-pads which acted as the source and drain electrodes. The Si substrate was used as the back gate electrode (Fig 1(c)). Conductance measurements as a function of the gas environment and temperature were carried out on isolated individual nanowires in a custom-designed 100 ml gas cell.

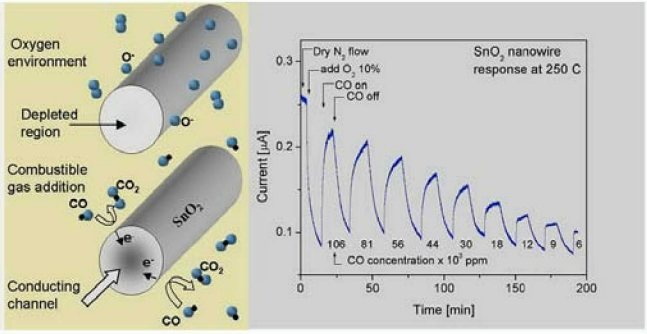

Figure 3. Single-nanowire gas sensor. The conductance response of the SnO_2 nanowire to O_2 and CO gases admitted into an inert (N_2), flowing atmosphere.

2.2 Nanowire Chemoresistors

Because of the large surface-to-bulk ratio and the fact that the nanowire's radius (~30 nm) is comparable or less than the Debye length for SnO_2 in the temperature range used, one can expect the nanowire's electronic and transport properties to be strongly, indeed primarily, affected by surface processes involving electron exchange between the surface and the adsorbate. The SnO_2 nanowires studied showed significant conductance changes when exposed to oxidizing and reducing gases[27] (Fig. 3). Under these so-called "flat band" conditions, the electrons are distributed homogeneously throughout the entire volume of the nanowire. The facile access of bulk electrons at the surface (and vise versa) and their limited number, causes the charge density throughout the entire nanowire to decrease or increase as a result of charge transfer processes occuring at its surface. For SnO_2 at ~600 K, the material's high conductance under inert or reducing atmospheres (Fig.3) results from the presence of shallow, i.e. totally ionized, donor states which arise as a result of surface-oxygen vacancies. This also renders the oxide an n-type semiconductor. Under these conditions the Fermi level lies just below the conduction band edge (Fig.4(a)). Exposure to oxygen saturates the surface vacancies, drawing electrons from the bulk, localizing them on the ionically-adsorbed (ionosorbed) oxygens (right panel of the Fig. 4(a)) according to the reaction:

$$\beta \cdot O_2^g + \alpha \cdot e^- + S \rightarrow O_{ads}^{-\alpha} \qquad (1),$$

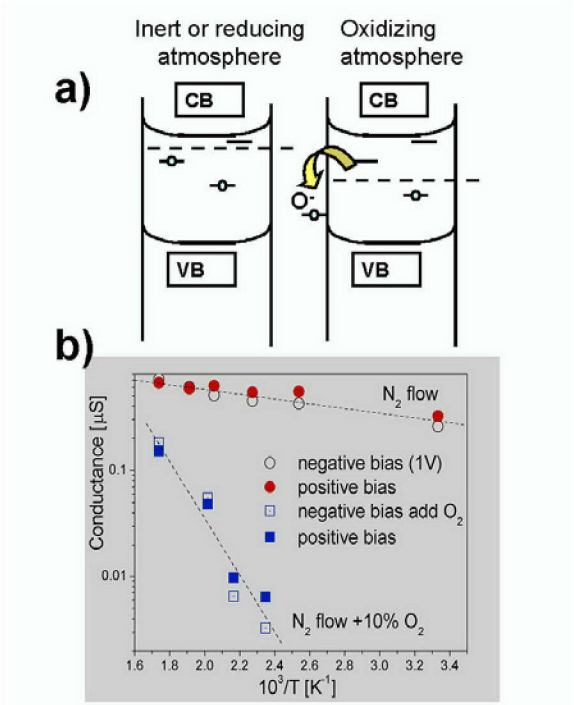

Figure 4. Effect of oxygen ionosorption on the electronic structure of a semi-conductor nanowire resulting in depletion of shallow donor states (a). The latter is reflected in an adsorbate-induced increase in conductance activation energy (b)

where the indices *g* and *s* indicate gas and surface, respectively; while β, α determine the molecular and charge status of the adsorbed oxygen. *S* designates an adsorption site.[28] In larger systems (i.e. when the nanowire's diameter, $D>>\lambda_D$) oxygen chemisorption induces band bending only near the surface. By contrast, in nanowires for which $D<\lambda_D$ adsorption can shift the Fermi level of the entire nanowire (Fig.4(a)), and the consequent electron depletion can result in a significant drop in conductance (Fig. 3, 4(b)) and a corresponding increase in activation energy (Fig.4 (b)).[27] A combustible gases such as CO reacts with previously-adsorbed or co-adsorbed oxygen to form CO_2 catalytically (according to the reaction shown below), thereby reducing the steady state surface oxygen concentration whose eletrons are donated back to the nanowire. This increases its conductivity significantly[28]:

$$\beta \cdot CO^{g\,or\,S} + O^{-\alpha}_{\beta S} \rightarrow \beta \cdot CO^{g}_{2} + \alpha \cdot e^{-} + S \qquad (2)$$

In this process, the CO-induced current recovery (Fig. 3) is proportional to the reduction in the coverage of ionically adsorbed oxygen. The electron exchange occurring in reactions (1) and (2) comprise the principle of operation of nanowire chemoresistor sensors for oxidizing and reducing adsorbates. In a "real world" environment a large number of other molecules (chief among them, water) complicates the picture. Surface hydroxyls and hydrocarbons can temporarily or permanently react with adsorption sites modifying or adding to the possible reaction pathways.

2.3 Nanowire Field Effect Transistors And Surface Reactivity

The architecture of a typical nanowire-based FET is shown in Fig. 1(c) and 5(a)). The nanowire acts as a conducting channel connecting a source (S) and drain (D) electrode. The entire assembly rests on a thin oxide film, which itself lies on top of a conducting (in this case p-type Si) gate (G) electrode. Most of the SnO_2 nanowires studied showed a prominent gate effect (Fig.5c) as an n-channel FET. As with chemoresistors, the FET's performance is affected by the composition of ambient gas (Fig. 5(d)) and temperature.[27] Under dry nitrogen (and after several hours' annealing) the

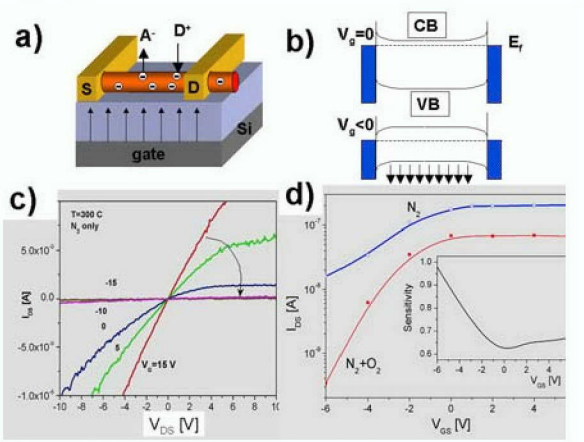

Figure 5. The architecture (a), principle (b), and performance (c) of a nanowire-based FET under nitrogen and oxygen/nitrogen gaseous atmospheres (d).

nanowire becomes a fairly good conductor, whose conductivity depends only moderately on gate potential (top curve in Fig.5d). The switching ratio under these conditions was only 5-10, due to screening by conduction electrons whose high density prevented the gate field from modulating the current significantly. In the presence of oxygen, and with a sufficiently negative gate potential, V_{GS}, the reduced electron density magnifies the effect of the gate potential enormously, resulting in efficient switching of the source-drain current (I_{DS}) and a positive shift in the threshold value of the FET's transfer function (Fig. 5d, bottom curve). The highest switching ratios (~10^3) were observed in air at room temperature for vapor grown SnO_2 nanowires. Although large, this value is lower than the record value of 10^4 reported for nanobelts[4]. Based on this observation, the sensitivity, $S= (G_0-G_{oxy})/G_0$, of the nanowire configured as an FET and operating as an oxygen sensor can also be maximized by tuning the gate potential to the threshold voltage appropriate to the specific gas being probed.

2.4 The Influence Of Gate Potential On The Catalytic Performance Of A Nanowire

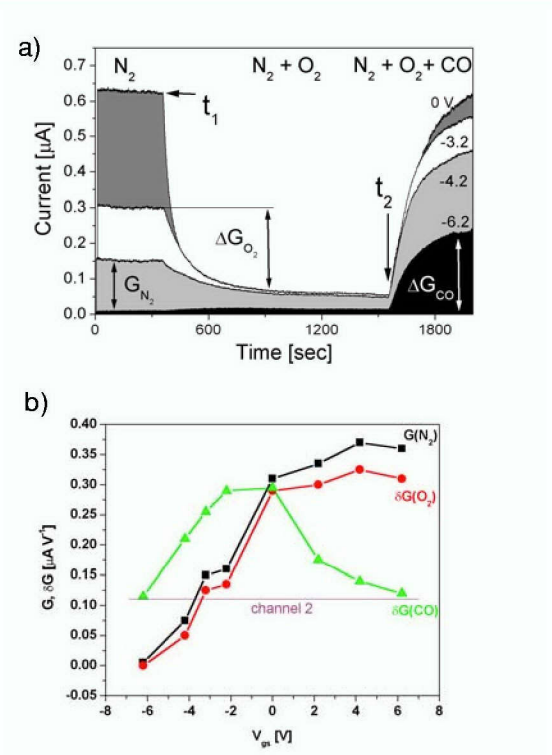

Figure 6.
(a) Response of the nanowire's source-drain current (V_{SD}=2 V) to the sudden addition of 10 sccm of oxygen to the (100 sccm) of flowing nitrogen gas at time t_1 followed by the addtion of 5 sccm of CO at time t_2 at various values of the gate potentials at 553 K. The quantity G_{N2} is I_{SD} under nitrogen. $\Delta G_{O2(CO)}$, the values of the conductance decrease (increase) when O_2 (CO) gas is sequentially admitted into the gas cell. (b) The reactivity of oxygen, ΔG_{oxy}, and CO, ΔG_{CO}, as a function of gate voltage as measured by the total change in conductance determined from the response curves shown in Fig. 6a. The nanowire conductance G_{N2} under dry nitrogen is included for comparison. Also shown: the extent of reaction of CO through a putative second reaction channel that does not involve ionosorbed oxygens as a reagent.

The ability to shift almost continuously the position of the Fermi level of an oxide nanowire configured as FET by varying its gate potential (Fig. 5(b)) can, in principle, allow molecular adsorption onto its surface to be controlled. Because ionosorbed oxygen is a precursor to many catalytic reactions like CO oxidation, one expects the extent, rate and selectivity of catalytic reactions occurring on the nanowire's surface to be, likewise, gate-voltage controllable. The interplay between adsorption, electron transport, catalysis and gate voltage in an FET-configured SnO_2 nanowire were explored. Illustrating the results, the variation of I_{SD} at V_{SD}= 2 V as a function of gas partial pressures at various gate potentials are shown in Fig. 6a. The baseline I_{DS} is taken to be its steady state value, measured following prolonged exposure to dry N_2 at the selected gate potential and temperature. On changing V_{GS} to a new value the system was allowed to sit under dry nitrogen a sufficiently long time for steady state to be re-established. At time t_1, 10 sccm of oxygen gas was mixed into the 100 sccm nitrogen flow. This was followed at time t_2 by the addition of CO (5 sccm) into the gas flowing into the cell.

A number of observations can be deduced from the data presented in Fig 6a.

(i) The steady-state value of the conductance in the nitrogen atmosphere decreases monotonically when gate potential becomes more negative and drops by a factor ~ 70 times at V_{GS} = -6 V. With increasing the positive gate potential the conductance increases somewhat then saturates.

(ii) The extent of the conductance drop upon oxygen admission decreases as V_{GS} becomes more negative. When V_{GS} =-6 V the conductance no longer changes on admitting oxygen. Assuming the conductance decrease on exposure to oxygen is proportional to the coverage of ionosorbed oxygen, a sufficiently negative gate potential can reduce I_{DS} to zero (Fig. 6(a) bottom curve) suggesting that ionosorption no longer takes place (although physisorbed oxygen may still be present on the surface).

(iii) The increase in conductance on admitting CO, which we ascribe to the effect of catalytic oxidation of CO, begins almost immediately upon the introduction of CO achieving steady state slowly. The increase in conductance is not a monotonic function of the gate potential reaching a maximum value when V_{GS} is in the range –2 to 0 V.

(iiii) Interestingly, CO admission increases the conductance at V_{GS} = -6 V, although ionosorbed oxygen is presumably absent.

The concomitant dependence of ΔG_{oxy} and $G(N_2)$ on gate voltage shown in the Fig. 6b is immediately understandable by noting that tin dioxide is an n-type semiconductor. Negative values of the gate voltage decrease the electron density in the nanowire thereby decreasing its conductance G_{N2}. Because the ionosorption of oxygen on the nanowire makes use of, and localizes electrons derived from the bulk of the nanowire onto the surface oxygens, as the electron concentration decreases so will the capacity for ionosorption of oxygen. In fact, because the electron can be regarded as a reagent in the ionic chemisorption process, and oxygen is in excess, the extent of oxygen chemisorption (ΔG_{oxy}) should track the carrier concentration exactly, which is precisely what is found. Because the nanowire's surface to volume ratio is very large (there are only some 10^7 carriers in the nanowire) it is easy to attain fields strong enough even at low values of the gate voltage to reduce the carrier concentration to essentially zero, shutting down the oxygen chemisorption

process and all subsequent surface processes in which ionically chemisorbed oxygen is a reactant.

For positive values of the gate voltage both ΔG_{oxy} and G_{N2} are found to increase slightly with increasing gate voltage, eventually reaching a plateau possibly signifying the fact that the saturation electron density of the nanowire has been reached.

The range of options CO has for reacting with SnO_2 is more elaborate than oxygen, leading to the observed amonotonic dependence of the nanowire's conductance on the gate potential when CO is present in the gas mixture. Taking our cues from the well-established CO sensing mechanism developed for the thin film sensors,[28] we assume that the current recovery following the admission of CO, ΔG_{CO}, is proportional to the reduction in ionosorbed oxygen coverage, which is consumed in the catalytic CO oxidation reaction (2) to form CO_2. An important and reproducible feature of the reaction with CO is a significant increase in I_{SD} even at very negative values of the gate potential where oxygen ionosorption was completely shut down (see, e.g. ΔG_{CO} at V_{GS} = -6 V in Fig. 6 (a)). This more complicated behavior can be reconciled if one assumes that there are at least two CO reaction channels. The second channel can be ascribed to CO reduction of the lattice oxygens of the SnO_2 as opposed to the ionosorbed surface oxygens or hydroxyl groups. (There may also be some contribution due to charge donation by CO itself adsorbed at metal sites with unsatisfied valences, as in carbonyls, or through other reaction intermediates with Lewis base character formed subsequent to adsorption.) When a mixture of CO and oxygen simultaneously fed into the chamber the conductance change will reflect the sum of contributions from all of the surface processes, which proceeds with electron exchange with the nanowire. Let us consider the three following processes: (A) the interaction of CO molecules with the lattice oxygen. This reaction channel would likely not affect the electron density and therefore will, therefore, not be affected by the gate potential; (B) The interaction of CO with ionosorbed oxygen, which depends on the availability of free electrons and therefore on gate voltage and (C) the ionosorption of oxygen itself which also changes with the gate potential as noted above. At steady state (conductance, temperature and gas composition and pressure), and making these assumptions, the ionosorbed oxygen coverage, $\theta(V_{GS})$, can be deduced.[29] The result of such an analysis is shown in Fig. 7 which plots the ionosorbed oxygen coverage as a function of the gate potential before and after CO is admitted into the flowing N_2+O_2 mixture. The most notable effect of CO reacting with the surface oxygens is to shift the steady-state oxygen coverage to lower values at any given value of V_{GS}. At the most negative values of V_{GS}, the combined effect of a low electron density and the surface reactivity of CO is to essentially eliminate ionosorbed oxygen from the surface of the nanowire (triangles in the Fig.7). Contrariwise, when electrons (and therefore ionosorbed oxygen) become plentiful (at positive values of V_{GS}, the impact of CO reactivity decreases, eventually to the point where its effect on the steady-state ionosorbed oxygen coverage becomes negligible even with CO present. This immediately explains the amonotonic evolution of $\Delta G_{co}(V_g)$ in Fig. 6b. At negative values of V_{GS} below a threshold vale, V_{th}, the conductance increase is almost solely determined by the reaction of CO with lattice oxygens. As the gate potential is increased, more ionosorbed oxygens survive

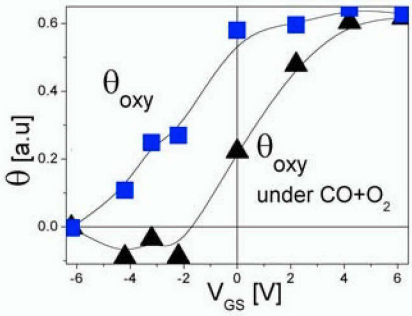

Figure 7. The dependence of the calculated steady-state oxygen coverage on gate potential before (squares) and after (triangles) CO gas is admitted.

exposure to CO and $\Delta G_{co}(V_g)$ reaches a maximum then decreases again at a high enough, positive value of V_{GS}. At this point the steady-state oxygen coverage with or without CO present in the gas flow is almost equal. This behavior can be accounted for by assuming that both CO and oxygen compete for the same sites on the nanowire's surface. At negative values of V_{GS}, few oxygens adsorb because few electrons are available, leaving lots of room for CO to adsorb. However, these COs have few reaction partners on the surface with which to react (other than through the second channel). As the gate potential is increased, more oxygen molecules ionosorb on the surface providing an increasing number of reaction partners for the co-adsorbed COs. With further increase in gate potential more ionosorbed oxygens accumulate on the surface eventually reducing the number of sites available for CO co-adsorption, at which point CO reactivity (through channel 1) reaches a maximum. With further increase in gate potential the extent of CO reactivity begins to decline as a result of the shortage of adsorbed CO molecules. All the while, reaction through channel 2 takes place in a V_{GS}-independent process (Fig. 6b).

The above conclusions are supported by the analysis that was carried out on the experimental reaction kinetics[30] assumed to be reflected in the response if the current I_{SD}. These analyses were carried out independently on the decreasing and increasing portions of the current evolution with time following, respectively, the addition of oxygen, then oxygen+CO, to

the flowing nitrogen (Fig. 6a). Briefly, we found that at the most negative values of the gate potential the time evolution of I_{SD} was adequately reproduced by a single exponential. Beyond a certain value of the gate potential the time evolution of I_{SD} could only be adequately fit with a sum of two exponentials. Remarkably, one of the rate constants (beyond this value of the gate voltage) was essentially independent of gate potential and approximately equal in value to the value retrieved in the single exponential regime, while the second rate constant showed a marked dependence on gate potential.

The above two-channel model of CO oxidation has an interesting implication for the use of nanowires as catalysts. In essence we have shown that one can dramatically alter the branching ratio of the nanowire's catalytic action in the CO oxidation reaction simply by changing the gate potential under unchanging conditions of temperature, reactant composition and pressure.

3. SUMMARY AND CONCLUSIONS

In summary, the electron transport properties of individual, n-type semiconductor tin oxide nanowires were determined over a wide range of temperature and gas composition, with the nanowire configured alternatively as chemoresistors and FETs. Because of their large surface to volume ratios, the bulk electronic properties of the nanowires were found to be controlled almost entirely by processes taking place at their surface which could, in turn, be modified by controlling the gate potential. As a result, the rate and extent of oxygen ionosorption and the resulting rate and extent of catalytic CO oxidation occurring at the nanowire's surface could be controlled and even entirely halted by applying a negative enough gate potential. The above results suggest an intriguing strategy for producing nano-catalysts with electrically-tunable reactivity and selectivity according to the value of the gate potential. For example, for a nanowire at whose surface two reactions are possible, one can envision setting the gate potential as a chemical potential set-point so as to reduce one of these channels with respect to the other (assuming the two reactions differ somewhat in their redox properties). The nanowire FET then becomes, in essence, a nano-reactor with electronically controllable selectivity. Likewise, one can foresee using this effect to observe and control catalytic activity on supported metal particles. Even a small metal particle would normally contain sufficient numbers of electrons to fully support the metal-adsorbate charge exchange accompanying a catalytic reaction on its surface. Under ordinary circumstances, therefore, the charge exchange between the metal particle and its metal-oxide support would be negligible. However, if the support were a metal oxide nanowire configured as an FET, the gate potential could, in principle, induce the metal-adorbate charge transfer to include the nanowire and hence to be observable through the source-drain current. This would constitute a novel way for following catalytic processes occurring at supported metal catalyst particles. Alternatively, by controlling the gate potential one could manipulate a catalytic reaction occurring on the metal particle's surface.

4. ACKNOWLEDGMENTS

This work made extensive use of the MRL Central Facilities at UCSB supported by the National Science Foundation under award No. DMR-0080034 and DURINT-AFOSR Air Force Office of Scientific Research under DURINT grant F49620-01-1-0459

5. REFERENCES

(1) Huang, M. H.; Mao, S.; Feick, H.; Yan, H. Q.; Wu, Y. Y.; Kind, H.; Weber, E.; Russo, R.; Yang, P. D. *Science* 2001, *292*, 1897-1899.

(2) Pan, Z. W.; Dai, Z. R.; Wang, Z. L. *Science* 2001, *291*, 1947-1949.

(3) Comini, E.; Faglia, G.; Sberveglieri, G.; Pan, Z. W.; Wang, Z. L. *Applied Physics Letters* 2002, *81*, 1869-1871.

(4) Arnold, M. S.; Avouris, P.; Pan, Z. W.; Wang, Z. L. *Journal of Physical Chemistry B* 2003, *107*, 659-663.

(5) Wu, Y. Y.; Yan, H. Q.; Yang, P. D. *Topics in Catalysis* 2002, *19*, 197-202.

(6) Li, C.; Zhang, D. H.; Han, S.; Liu, X. L.; Tang, T.; Zhou, C. W. *Advanced Materials* 2003, *15*, 143-+.

(7) Collins, P. G.; Bradley, K.; Ishigami, M.; Zettl, A. *Science* 2000, *287*, 1801-1804.

(8) Kong, J.; Franklin, N. R.; Zhou, C. W.; Chapline, M. G.; Peng, S.; Cho, K. J.; Dai, H. J. *Science* 2000, *287*, 622-625.

(9) Kong, J.; Chapline, M. G.; Dai, H. J. *Advanced Materials* 2001, *13*, 1384-1386.

(10) Cui, Y.; Wei, Q. Q.; Park, H. K.; Lieber, C. M. *Science* 2001, *293*, 1289-1292.

(11) Law, M.; Kind, H.; Messer, B.; Kim, F.; Yang, P. D. *Angewandte Chemie-International Edition* 2002, *41*, 2405-2408.

(12) Li, C.; Zhang, D. H.; Liu, X. L.; Han, S.; Tang, T.; Han, J.; Zhou, C. W. *Applied Physics Letters* 2003, *82*, 1613-1615.

(13) Gopel, W. *Sensors and Actuators* 1989, *16*, 167-193.

(14) Sberveglieri, G. *Sensors and Actuators B-Chemical* 1992, *6*, 239-247.

(15) Yamazoe, N.; Miura, N. *Sensors and Actuators B-Chemical* 1994, *20*, 95-102.

(16) Moseley, P. T. *Measurement Science & Technology* 1997, *8*, 223-237.

(17) Kohl, D. *Journal of Physics D-Applied Physics* 2001, *34*, R125-R149.

(18) Hellmich, W.; Muller, G.; Bosch-Von Braunmuhl, C.; Doll, T.; Eisele, I. *Sensors and Actuators B-Chemical* 1997, *43*, 132-139.
(19) Scharnagl, K.; Bogner, M.; Fuchs, A.; Winter, R.; Doll, T.; Eisele, I. *Sensors and Actuators B-Chemical* 1999, *57*, 35-38.
(20) Lakshmi, B. B.; Dorhout, P. K.; Martin, C. R. *Chemistry of Materials* 1997, *9*, 857-862.
(21) Masuda, H. *Electrochemistry* 2001, *69*, 879-883.
(22) Routkevitch, D.; Tager, A. A.; Haruyama, J.; Almawlawi, D.; Moskovits, M.; Xu, J. M. *Ieee Transactions on Electron Devices* 1996, *43*, 1646-1658.
(23) Metzger, R. M.; Konovalov, V. V.; Sun, M.; Xu, T.; Zangari, G.; Xu, B.; Benakli, M.; Doyle, W. D. *Ieee Transactions on Magnetics* 2000, *36*, 30-35.
(24) Nicewarner-Pena, S. R.; Freeman, R. G.; Reiss, B. D.; He, L.; Pena, D. J.; Walton, I. D.; Cromer, R.; Keating, C. D.; Natan, M. J. *Science* 2001, *294*, 137-141.
(25) Kolmakov, A.; Zhang, Y.; Moskovits, M. *Nano Letters* 2003, *3 :*, 1125-1129.
(26) Dai, Z. R.; Gole, J. L.; Stout, J. D.; Wang, Z. L. *Journal of Physical Chemistry B* 2002, *106*, 1274-1279.
(27) Kolmakov, A.; Zhang, Y.; Cheng, G.; Moskovits, M. *Advanced Materials* 2003, *15*, 997-1000.
(28) Barsan, N.; Weimar, U. *Journal of Electroceramics* 2001, *7*, 143-167.
(29) Kolmakov, A.; Moskovits, M. *Ann. Rev. Mater. Res.* 2004, *34*, 151-80.
(30) Zhang Y.; Kolmakov A.; Metiu H.; S., C.; Moskovits M. *Nano Letters* 2003, *3*, 1125.